RESEARCH ARTICLE

[M] macro-olecular
Rapid Communications
www.mrc-journal.de

Toughening of Bio-Based PA 6.19 by Copolymerization with PA 6.6 – Synthesis and Production of Melt-Spun Monofilaments and Knitted Fabrics

Maximilian Rist, Henning Löcken, Mathias Ortega, and Andreas Greiner*

This work reports on the synthesis of statistical copolymers of bio-based PA 6.19 and PA 6.6 together with the production of melt-spun monofilaments for the production of sustainable textile fibers. The plant oil-based 1.19-nonadecanedioic acid is synthesized from bio-derived oleic acid via isomerizing methoxycarbonylation. The homopolymer PA 6.19 with a carbon-based bio-content of 72% shows a good elongation at break of 166%, but lower tensile strength than commercial PA 6 (43 MPa versus 82 MPa). Addition of adipic acid to form statistical PA 6.6/6.19 copolymers improves toughness while maintaining the high elongation at break. Two PA 6.6/6.19 copolymers with a carbon-based bio-content of 26% and 33% are successfully synthesized and exhibited comparable toughness (94 $\pm$ 6 MPa and 92 $\pm$ 2 MPa) to the commercial PA 6 (92 $\pm$ 15 MPa). The bio-based copolymers also exhibit a much lower water uptake than PA 6 and PA 6.6, resulting in a higher dimensional stability. Melt spinning of the oleic acid-based polyamides is successfully carried out to produce monofilaments with sufficient properties for further processing in a knitting process, demonstrating the capabilities of the bio-based PA 6.6/6.19 copolymers for use in the textile industry.

1. Introduction

The need for sustainable materials is greater than ever. With the European Union's goal of being carbon neutral by 2050, extensive research needs to be done in various areas to achieve this goal.[1] The global fiber industry, for example, produced about 70 million tons of synthetic fibers in 2020, of which less than 0.5% came from renewable sources.[2] This is mainly due to the high prices and low availability of bio-based materials. A particularly important material for the production of synthetic fibers is polyamide (PA), with an annual production volume of over 5 million tons.[2] Only about 0.4% of these polyamides are produced from bio-based raw materials, which are mostly ricinoleic acid. Since castor beans are the only economically viable feedstock for ricinoleic acid, the production of bio-based polyamides depends heavily on this one feedstock.[3] Expanding the available feedstocks would increase the availability of bio-based raw materials for polyamides and consequently lower prices, making the production of bio-based polyamides more economically viable. Oleic acid, for example, can be found in almost all natural fats and oils, and is thus readily available. Despite the structural similarity to ricinoleic acid, new synthesis methods need to be developed for the valorization of oleic acid for the synthesis of polymers for synthetic fibers.

Polyamide-based textile fibers are usually produced by melt spinning, where high crystallinity of the polymers is advantageous.[4] Linear polyamides without side chains are therefore the preferred choice. Numerous synthesis strategies for oleic acid-based monomers such as linear diacids,[5–7] amino acids,[6,8] and lactams[9] have been developed in recent years. However, the actual synthesis of the oleic acid-based polyamides via these linear amino acids and lactams[10] has often not been described so far. In contrast, the synthesis of linear polyamides from oleic acid-based diacids was described for PA X.9,[11] PA X.11,[12] PA X.18,[13] and PA X.19.[5,14]

The processing of oleic acid-based polyamides has been described mainly for extruded films for food packaging.[15] Melt-spun textile fibers from oleic acid-based polyamides have not been described yet. Recently we investigated the mechanical properties of PA X.19 and they showed good melt processability.[16] However, they exhibited significantly lower tensile strength compared to commercial polyamides such as PA 6. Copolymerization with a tougher material like PA 6.6 could potentially increase the tensile strength and ultimately create a partially bio-based material with comparable or better properties than commercial PA 6. Similar approaches have been

M. Rist, A. Greiner
University of Bayreuth
Macromolecular Chemistry and Bavarian Polymer Institute
Universitätsstrasse 30, 95440 Bayreuth, Germany
E-mail: greiner@uni-bayreuth.de
H. Löcken, M. Ortega
RWTH Aachen University
Institut fuer Textiltechnik
Otto-Blumenthal-Strasse 1, 52074 Aachen, Germany

Table 1. Feed ratio, yields and molecular weight of the copolymers PA 6.6/6.19, their homopolymers PA 6.6 and PA 6.19 and the benchmark PA 6.

Polyamide	Feed PA 6.6/PA 6.19 [mol%]	Experimental[a] [mol%]	Yield [%]	M_n[b]	M_w[b]	$Đ$[b]	Bio-content[c] [%]
PA 6 (benchmark)				34 900	58 500	1.7	0
PA 6.19	0/100	0/100	92	28 600	57 100	2.0	72
PA 6.6/6.19 17:83	17/83	17/83	93	30 200	52 400	1.7	60
PA 6.6/6.19 31:69	31/69	31/69	90	29 500	56 600	1.9	50
PA 6.6/6.19 44:56	44/56	44/56	91	44 100	82 400	1.9	41
PA 6.6/6.19 55:45	55/45	54/46	77	30 600	62 000	2.0	33
PA 6.6/6.19 64:36	64/36	64/36	79	48 700	93 200	1.9	26
PA 6.6/6.19 88:12	88/12	87/13	80	49 200	110 100	2.2	9
PA 6.6	100/0	100/0	92	59 500	118 600	2.0	0

[a] Calculated by ^{1}H-NMR spectroscopy, [b] SEC (HFIP + 0.1% KTFA, room temperature, PMMA-standard), [c] The percentage of bio-based carbon content of the total carbon content in accordance with DIN EN 16 640.

described for the toughening of PA 11 by in situ polymerization with PA 6.6,[17] as well as copolymerization of dimer oleic acid-based PA 6.36 with PA 6.6[18,19] or PA 11 with PA 6.[20] An increasing tensile strength was observed with increasing PA 6.6 or PA 6 content in the copolymer.

Herein, we report on the synthesis of bio-based copolymers of oleic acid-based PA 6.19 and PA 6.6. The copolymers were synthesized via melt polycondensation from mixtures of the respective PA-salts to obtain statistical copolymers with molecular weights in the range of common engineering polyamides (≈30 000). Full characterization of the thermal, viscoelastic and mechanical properties of the resulting copolymers was performed by differential scanning calorimetry (DSC), thermogravimetric analysis (TGA), dynamic mechanical analysis (DMA), plate-plate rheology and uniaxial tensile testing. The best performing copolymer formulation was synthesized in a larger scale and melt-spun into monofilaments. In addition, the fineness and the mechanical properties of the monofilaments were characterized. Finally, a knitted fabric was produced from the monofilaments supporting their suitability for the production of oleic acid-based textiles.

2. Results and Discussion

2.1. Synthesis of PA 6.6/6.19 Copolymers

The PA 6.6/6.19 copolymers were synthesized by mixing PA-salts of PA 6.19 and PA 6.6 in the desired ratio. The polymerization was then carried out via melt polycondensation in two steps. At the beginning oligomers were formed in a precondensation step by gradually increasing the temperature from 160 to 260 °C. Then the main polycondensation was performed at 260–280 °C with later application of vacuum. After 8–9 h of reaction time the synthesis was aborted and the polymers were received as white and off-white solids via precipitation in good yields of up to 93% (**Table 1**).

The number average molecular weight (M_n) of the final polymers ranged from 28 600–59 500, meeting the range of the PA 6 benchmark (34 900) and that of common technical grade polyamides (Table 1). Surprisingly, an increasing molecular weight with increasing PA 6.6 content was observed. A similar observation was made during the copolymerization of PA 11

and PA 6.[20] It was assumed that the higher hydrophilicity of ϵ-caprolactam inhibits the removal of water during the polycondensation resulting in lower molecular weights for copolymers with high PA 6-content. However, we observed an increasing molecular weight with increasing hydrophilicity of the copolymers, indicating a different cause.

2.2. Thermal Properties

Analysis of the thermal properties of the polyamides was performed via TGA and DSC. The corresponding data are given in **Table 2**. The thermal stability of the polyamides was observed by TGA under synthetic air and nitrogen atmosphere. All synthesized polyamides showed high thermal stability with a 5% degradation temperature ($T_{5\%}$) of >395 °C under nitrogen and air atmosphere, showing single-stage degradation. Additionally, the thermal stability of the synthesized copolymers at their respective processing temperature was investigated using isothermal TGA analysis. Here, all polyamides showed high stability with a mass loss of less than 1.4% under nitrogen atmosphere. Under air atmosphere the polyamides processable below 270 °C (PA 6.19, PA 6.6/6.19 17:83, 31:69, 55:45) showed again a high thermal stability with a maximum mass loss of 0.5% under air. Processing at higher temperatures led to a mass loss of 1.4% to 4.3% under air atmosphere. The exclusion of oxygen is therefore crucial during processing in order to minimize thermal decomposition of the material.

The melting and crystallization behavior of the polyamides were studied by DSC. Both the melting temperature (T_m) and the crystallization temperature (T_c) of the copolymers showed a strong dependence on the PA 6.6 content (**Figure 1**). Initially, the melting temperature decreased with increasing PA 6.6 content from 190 °C for the PA 6.19 homopolymer to 177 °C for the copolymer with 31 mol% PA 6.6. From then on, the melting temperature increased in an almost linear trend with the PA 6.6 content to 259 °C for the PA 6.6 homopolymer. A similar trend was observed for the crystallization temperature, with 174 °C for PA 6.19 to 142 °C for the 31:69 copolymer and from there to 216 °C for PA 6.6. This is typical for statistical copolymers and is due to the disruption of the crystal structure by the

2300256 (2 of 11)

ADVANCED
SCIENCE NEWS

www.advancedsciencenews.com

⌈M⌉ **acro-**
olecular
Rapid Communications

www.mrc-journal.de

Table 2. Thermal Properties of the Polyamides.

Polyamide	TGA				DSC				DMA
	Nitrogen		Air		Second heating		Cooling		Second heating
	$T_{5\%}$ [a] [°C]	Mass loss at $T_{process}$ [b] [%]	$T_{5\%}$ [a] [°C]	Mass loss at $T_{process}$ [b] [%]	T_m [c] [°C]	ΔH_m [c] [J g^{-1}]	T_c [b] [°C]	X_c [d] [%]	T_g [e] [°C]
PA 6 (benchmark)	406	0.9	404	0.5	219	64	153	34	
PA 6.19	444	0.1	414	0.0	190	86	174	44	59
PA 6.6/6.19 17:83	445	0.0	435	0.1	186	82	161	42	53
PA 6.6/6.19 31:69	415	0.3	397	0.4	177	70	142	35	52
PA 6.6/6.19 44:56	433	0.4	423	1.4	196	63	155	32	52
PA 6.6/6.19 55:45	433	0.3	409	0.5	209	42	161	21	49
PA 6.6/6.19 64:36	428	1.2	413	3.3	213	51	183	26	48
PA 6.6/6.19 88:12	422	1.0	411	2.6	248	56	202	28	63
PA 6.6	416	1.4	398	4.3	259	84	216	43	77

[a] $T_{5\%}$ is the temperature at 5% mass loss, measured at 20 K min^{-1}, [b] Mass loss after 1 h isothermal heating at their respective processing temperature ($T_{process}$), 210 °C for PA 6.19; 220 °C for PA 6.6/6.19 17:83 and 31:69; 270 °C for 44:56; 230 °C for 55:45; 280 °C for 64:36; 300 °C for 88:12 and PA 6.6, [c] Melting temperature (T_m), melting enthalpy (ΔH_m) and crystallization temperature (T_c) measured at a rate of ± 20 K min^{-1}, [d] Crystallinity (X_c) is calculated from $\Delta H_m / \Delta H_m^0$, with ΔH_m^0 being the enthalpy of fusion of 100% crystalline PA 6.6, 197 J g^{-1},[21] [e] Glass transition temperature (T_g) determined from the peak of the tan d measured at 2 K min^{-1}.
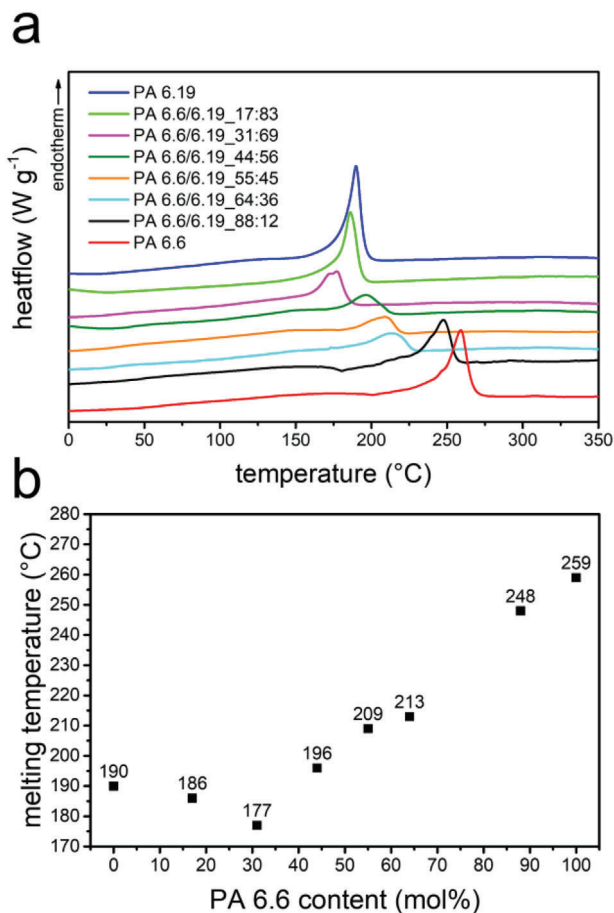
Figure 1. a) DSC thermographs of the synthesized polyamides. b) Determined melting temperatures of the polyamides as a function of the PA 6.6 content.
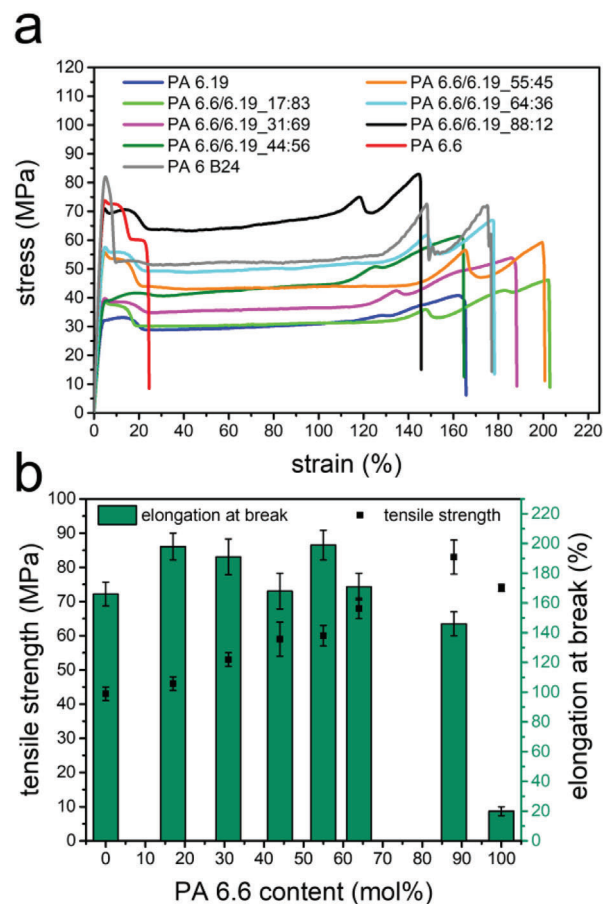
Figure 2. a) Stress–strain curves of synthesized polyamides and benchmark PA 6. b) Visualization of the tensile strength and the elongation at break in dependence of the PA 6.6 content. The error bar for the PA 6.6 homopolymer is too small to visualize.

**ADVANCED
SCIENCE NEWS**

www.advancedsciencenews.com

**[M]acro-
molecular
Rapid Communications**

www.mrc-journal.de

Table 3. Summarized mechanical properties of synthesized polyamides and benchmark PA 6.

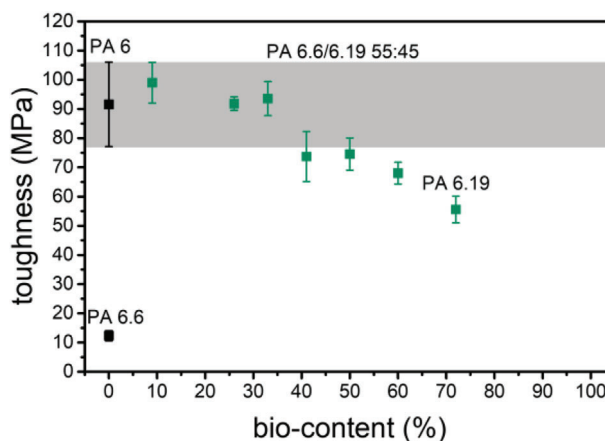| Polyamide	Young's modulus[a] [MPa]	Tensile strength[a] [MPa]	Elongation at break[a] [%]	Toughness[a] [MPa]	Water uptake[b] [%]
PA 6 (benchmark)	2200 ± 62	83 ± 3	170 ± 22	92 ± 15	11.33 ± 0.25
PA 6.19	1140 ± 16	43 ± 2	166 ± 8	56 ± 5	1.25 ± 0.03
PA 6.6/6.19 17:83	1220 ± 30	46 ± 2	198 ± 9	68 ± 4	1.86 ± 0.01
PA 6.6/6.19 31:69	1200 ± 25	53 ± 2	191 ± 12	75 ± 6	2.00 ± 0.02
PA 6.6/6.19 44:56	980 ± 60	59 ± 5	168 ± 12	74 ± 9	2.25 ± 0.00
PA 6.6/6.19 55:45	1460 ± 24	60 ± 3	199 ± 10	94 ± 6	2.38 ± 0.04
PA 6.6/6.19 64:36	1460 ± 34	68 ± 3	171 ± 9	92 ± 2	2.69 ± 0.03
PA 6.6/6.19 88:12	2160 ± 35	83 ± 5	146 ± 8	99 ± 7	4.91 ± 0.14
PA 6.6	2080 ± 61	74 ± 1	20 ± 3	12 ± 2	7.90 ± 0.05

[a] Measured in accordance with DIN EN ISO 527-2, at 50 mm min⁻¹ test speed [b] The water uptake is measured in deionized water at 25 °C for 7 d in accordance with DIN EN ISO 62.

addition of PA 6.6 units.[22] Consequently, a decrease in crystallinity was also observed with increasing PA 6.6 content. Starting from the homopolymer PA 6.19, the crystallinity decreased from 44% to 21% for the PA 6.6/6.19 55:45. Further increasing the PA 6.6 content resulted in an increase in crystallinity to 43% for the homopolymer PA 6.6. The local minimal crystallinity was therefore found with 55% PA 6.6, which is significantly higher than the local minimum found for the crystallization and melting temperature. Therefore, the effect of the increased frequency of amide-bonds already overweighs the disruption of the crystallinity. Similar behavior was also observed for the copolymers of polyamide 6 and 11.[20] In summary, the melting temperature of the PA 6.6/6.19 copolymers can be controlled by the PA 6.6 content. Up to 64 mol% PA 6.6, they also exhibit a lower melting temperature of 177–213 °C compared to the benchmark PA 6 (219 °C). The copolymers may therefore be processable at lower temperatures, which is beneficial in terms of energy consumption.

2.3. Mechanical Properties and Water Uptake

Uniaxial tensile tests were performed on injection molded specimens of the synthesized polyamides. The processing temperatures were adjusted according to the viscosities of the respective polymer sample to ensure processability and were in the range of 210–300 °C. The stress–strain curves can be observed in **Figure 2**a and the resulting values for the elongation at break and tensile strength are depicted in Figure 2b. The benchmark PA 6 showed an elongation at break of 170 ± 22% with a tensile strength of 83 ± 3 MPa. On the other hand, the bio-based PA 6.19 homopolymer showed a comparable elongation of 166 ± 8% but a significantly lower tensile strength of 43 ± 2 MPa (**Table 3**). This is, however, comparable to results obtained for similar long-chain polyamides such as PA 6.24 (33 MPa) and PA 6.34 (21 MPa)[23] and is likely due to the lower frequency of amide-bonds resulting in a lower amount of intermolecular hydrogen bonding.
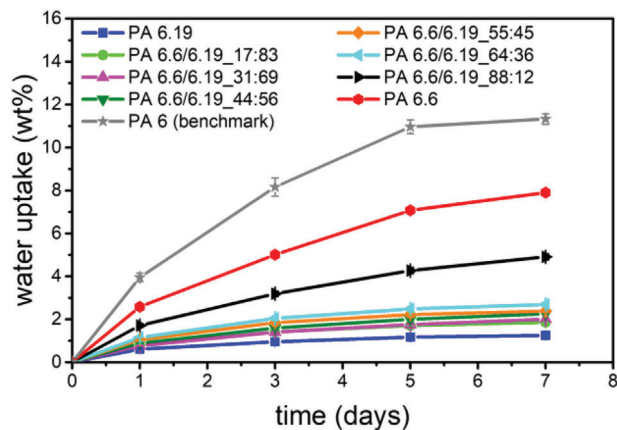
Increasing the PA 6.6 content in the copolymers resulted in an increase in both tensile strength and Young's modulus. Surprisingly, increasing the PA 6.6 content to 64 mol% did not affect the elongation at break, and all copolymers showed an elongation be-

Figure 3. Toughness of the polyamides against the bio-based carbon content.

tween 170–200%. Ultimately, the tensile strength was improved to 68 ± 3 MPa and the Young's modulus to 1460 ± 34 MPa, corresponding to an increase of 58% and 28%, respectively. However, these results are in contrast to prior findings for alloys and blends of PA 11 and PA 6.6, where both elongation at break and tensile strength increased with increasing PA 6.6 content for the alloys.[17] There was no effect on tensile strength in the blended samples, but the elongation at break decreased.[17] Increasing the PA 6.6 content to 10% in molecular composites of PA 6 and PA 66 also showed no effect on the tensile strength, but the elongation at break was drastically increased to 502%.[24] Copolymers of dimerized oleic acid-based PA 6.36 with PA 6.6, on the other hand, showed increasing tensile strength with PA 6.6 content, but a decrease in elongation at break.[18,19]

In **Figure 3**, the toughness of the synthesized polyamides together with the benchmark PA 6 is plotted against the bio-content as the percentage of bio-based carbon content in accordance with DIN EN 16 640. As the PA 6.6 content increases, the bio-content decreases since the carbon from the PA 6.6 is not bio-based. The toughness of the copolymers with a PA 6.6 content of 55, 64 and 88 mol% were all within the range of the benchmark PA 6 (92 ± 15 MPa). PA 6.6/6.19 55:45 showed the highest toughness of

ADVANCED
SCIENCE NEWS

www.advancedsciencenews.com

[M]acro-molecular
Rapid Communications

www.mrc-journal.de

Figure 4. Water uptake of the polyamides over time.

Figure 5. Temperature independent loss modulus versus storage modulus for the polyamides.

all synthesized polyamides with a bio-content of at least 20% (94 ± 6 MPa). In summary, the copolymers with 55 and 64 mol% PA 6.6 were synthesized as two sustainable alternatives with a bio-content of 33% and 26%, respectively, exhibiting comparable mechanical properties to the benchmark PA 6.

The water uptake of the copolymers was investigated by immersion in water and compared to the PA 6 benchmark, the resulting data can be observed in **Figure 4**. As expected, the benchmark PA 6 showed a high water uptake of 11.33 ± 0.25% after 7 days in deionized water. The copolymers, on the other hand, showed a significantly lower water uptake, which can be attributed to the higher hydrophobicity resulting from the long methylene chain of the PA 6.19 moieties. Consequently, the PA 6.19 homopolymer showed the lowest water uptake of 1.25 ± 0.03%, which is an order of magnitude lower than the benchmark PA 6. As the PA 6.6 content in the copolymers increased, the hydrophobicity decreased, which was evident in an increase of the water uptake to 7.90 ± 0.05% for the PA 6.6 homopolymer. Similar results were reported previously for branched oleic acid-based co-polyamides with PA 6.6.[25] Polymers having low water absorption are known to have higher dimensional stability, which in turn is advantageous for the production of melt-spun fibers and injection molded parts.[26] Owing to their low water uptake, the synthesized copolymers therefore offer significant advantages over PA 6 for melt processing applications.

2.4. Rheology

Important characteristics of a thermoplastic polymer suitable for melt spinning include sufficiently high molecular weight, thermal stability during processing, sufficient melt viscosity, high purity and high chain mobility.[27] All synthesized polyamides show high thermal stability with degradation temperatures ($T_{5\%}$) well over 100 K above their melting temperatures (Table 2). Their molecular weights (28 600–59 500) are also in the range of technical grade polyamides suitable for melt spinning like the benchmark PA 6 (34 900). The synthesized polyamides are also linear, which is favored due to their high chain mobility. In order to investigate on the potential spinnability of the synthesized polyamides their rheological properties were studied in the molten state.
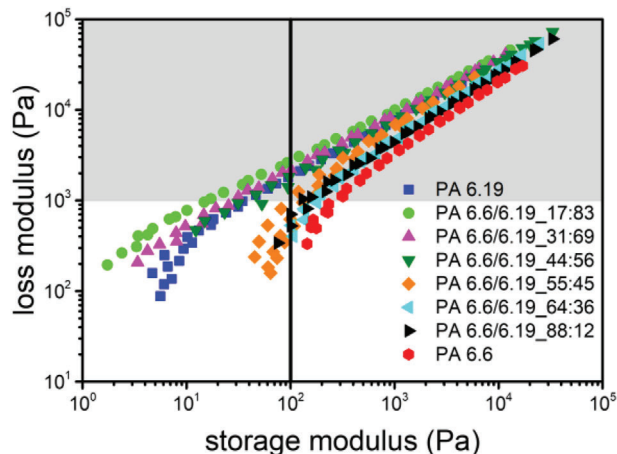
Frequency sweeps were recorded for all polyamides at three different temperatures between T_m + 10 K and T_m + 50 K at 2% deformation. The zero shear viscosity was then obtained by fitting the complex viscosity data from the rheology measurements. The Bird–Carreau–Yasuda model was chosen for fitting, as the model best described the measured data (Equation (2)).[28] With η_0 as the zero shear viscosity, $\dot{\gamma}$ as the share rate, n as the Power Law index, accounting for shear thinning, λ as a time constant and the parameter a controlling the curvature.
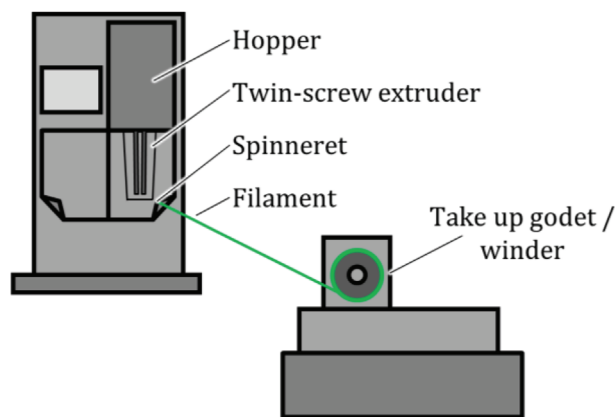
$$\eta\left(\dot{\gamma}\right) = \frac{\eta_0}{\left(1 + |\lambda\dot{\gamma}|^a\right)^{\frac{(n-1)}{a}}} \tag{1}$$

Construction of the temperature independent master curves could then be performed by calculation of the temperature shift factor $a_T(T)$. The master curves for all polymers can be found in Figures S8–S15, Supporting Information. Here, the Arrhenius shift was used, as this model is valid for semi-crystalline polymers such as the polyamides in this work (Equation (3)).[29] With T_0 being a reference temperature, T being a specific temperature and η_0 as the zero shear viscosity at the respective temperature obtained from the Bird–Carreau–Yasuda model (Equation (2)).

$$a_T\left(T\right) = \frac{\eta_0(T)}{\eta_0(T_0)} \tag{2}$$

Using these master curves, the spinnability of the polyamides can be estimated by plotting the loss modulus (G″) against the storage modulus (G′), and the resulting plots can be observed in **Figure 5**.

Previous studies have shown a correlation between the spinnability of commercial polyamides (PA 6, PA 4.6 and PA 6.6) and their rheological properties.[30] Polyamides with a G″ of at least 1000 Pa at a G′ of 100 Pa showed good spinnability, which deteriorated for polyamides with a lower G″. According to these results, the copolymers with a PA 6.19 content of at least 56 mol% should show good spinnability, as they all read a G″ of over 1000 Pa at the 100 Pa mark for G′ (indicated by the black line). Increasing the PA 6.6 content further seemed to result in

**ADVANCED
SCIENCE NEWS**

www.advancedsciencenews.com

**{M} acro-
molecular
Rapid Communications**

www.mrc-journal.de

Figure 6. Schematic drawing of the melt spinning process on the micro compounder used for the production of monofilaments.

a more elastic behavior of the polymer melt, indicating poorer spinnability. It was also observed that the PA 6.19 and PA 6.6/6.19 55:45 ceased to be thermo-rheological simple at lower shear rates, which is evident from the deviation of the individual measurements in the master curves in Figures S8 and S12, Supporting Information.

2.5. Melt Spinning

The PA 6.6/6.19 55:45 copolymer (CoPA) was produced in a larger scale of 70 g for the production of monofilaments by melt spinning. Polymerization was performed similar to the small-scale trials from the respective polyamide salt, just in a bigger tube. The final copolymer used for melt spinning had a number average molecular weight of 69 500 with a dispersity of 1.8 (size exclusion chromatography (SEC).

The most commonly used process for the production of man-made fibers is melt spinning. Here a polymer is either spun directly from the melt after polymer production (direct spinning) or polymer chips are produced first, and then melt-spun using an extruder (extruder spinning).[31] For extrusion spinning dried polymer chips are melted in an extruder at a specific temperature and transported to the spin head. A constant volume flow is ensured using a spin pump and the polymer melt is filtered and pressed through a spinneret containing one (monofilament) or multiple holes (multifilament). The resulting filaments are cooled by a constant air flow in the quench or with a tempered water bath. The filaments are drawn down by a take-up godet with a constant velocity. If a higher orientation of the polymer chains in the filaments is required, further drafting or drawing can be applied using more (heated) godets with higher rotational velocities. Eventually, the filaments are wound on a winder to receive a spool.[31] Melt spinning of CoPA and the commercial PA 6 was performed on a micro compounder and the resulting monofilament was taken up by a winder to receive spools (**Figure 6**).

Typical processing temperatures in melt spinning lie ≈40 K above the melting point of the polymer processed. Therefore, spinning trials of the commercial PA 6 and bio-based PA 6.6/6.19 55:45 were performed at 259 and 249 °C respectively. However,

the resulting viscosity of the polymer melt was too low, which resulted in an increased extrusion velocity to an extend that no winding was possible. Therefore, the extrusion temperature was adjusted to 240 °C for the commercial PA 6 and 225 °C for the bio-based copolymer. Monofilaments of both polymers were produced using different wind up speeds. The achieved draw-down ratios, as well as fineness, tenacity and elongation at maximum force can be observed in **Table 4**. The achieved draw-down ratios of up to 110 comply with industrial processing conditions for partially oriented yarns (POY) and thus prove the suitability of the material for industrial spinning tests.

Analysis of the produced monofilaments by scanning electron microscopy (SEM) revealed a smoother surface for the fibers spun from PA 6 (**Figure 7**). The surface of the filaments prepared from CoPA on the other hand showed grooves along the fiber. Increasing the wind up speed did not influence the formation of these grooves, the surface of the filament spun at 30 m min^{-1} and the one spun at 5 m min^{-1} look identical. For the commercial PA 6, however, a change in the surface morphology was observed for the monofilament spun at 30 m min^{-1}. Here, the surface is not as smooth as for the filaments spun at lower speeds. The filament developed so-called sharkskin, which is caused by a periodic adhesive failure of the polymer melt exiting the die at high velocities.[4]

For the bio-based CoPA a broad range of wind up speeds could be applied for the production of monofilaments. For both polyamides a general trend of decreasing fineness with increasing wind up speed was observed (Table 4, **Figure 8**a). The relatively high standard deviations are the result of manual determination of fineness and manual polymer feeding during the spinning process. Increasing the wind up speed also resulted in an increased tenacity of the monofilaments for both materials. This increase was more pronounced for PA 6, where increasing the wind up speed from 20 to 30 m min^{-1} resulted in a 40% increase in tenacity. The same increase in wind up speed did not result in a significant change in tenacity for the bio-based copolymer (Table 4, Figure 8b). On the other hand, the elongation at break at maximum force showed a decreasing trend with increasing wind up speed for the CoPA. No significant change in elongation was observed for the commercial PA 6 upon increasing the wind up speed from 20 m min^{-1} (Table 4, Figure 8b). These findings are in contradiction to earlier expectations, since an increase in tenacity and a decrease in elongation are normally accompanied by an increase in wind up speed. However, the high standard deviations due to manual feeding and determination of the fineness must be considered. No standard deviation is available for the copolymer wound at 40 m min^{-1} (CoPA_40), since not enough filament was produced during melt spinning and only the fineness of one piece could be determined.

2.6. Knitting Trials

In addition to melt spinning, the produced yarns are processed into textiles using the knitting process. Knitting is used for various applications such as t-shirts, socks, shoe-uppers or mattress covers. Since knitting can be generally performed with only one bobbin of material, the knitting process is often used to validate the further textile processing of the developed yarns. In the

ADVANCED
SCIENCE NEWS
www.advancedsciencenews.com

Macro-
molecular
Rapid Communications
www.mrc-journal.de

Table 4. Characteristics of monofilament spun from PA 6 and PA 6.6/6.19 (CoPA).

| Polyamide	Wind up speed [m min^{-1}]	Draw-down ratio	Fineness [dtex]	Tenacity [cN tex^{-1}]	Elongation at max. force [%]
PA 6_20	20	55.1	624 ± 69	10 ± 2	485 ± 23
PA 6_25	25	68.9	663 ± 89	10 ± 2	499 ± 23
PA 6_30	30	82.6	437 ± 161	14 ± 2	466 ± 13
CoPA_5	5	13.8	1146 ± 179	5.3 ± 1.2	164 ± 43
CoPA_10	10	27.5	1665 ± 131	5.0 ± 0.6	198 ± 16
CoPA_20	20	55.1	879 ± 253	6.9 ± 0.8	166 ± 27
CoPA_30	30	82.6	725 ± 247	7.3 ± 1.6	117 ± 31
CoPA_35	35	96.4	720 ± 199	7.5 ± 1.3	126 ± 18
CoPA_40	40	110.2	644[a]	-	-

[a] Only one measurement was possible, due to lack of material.
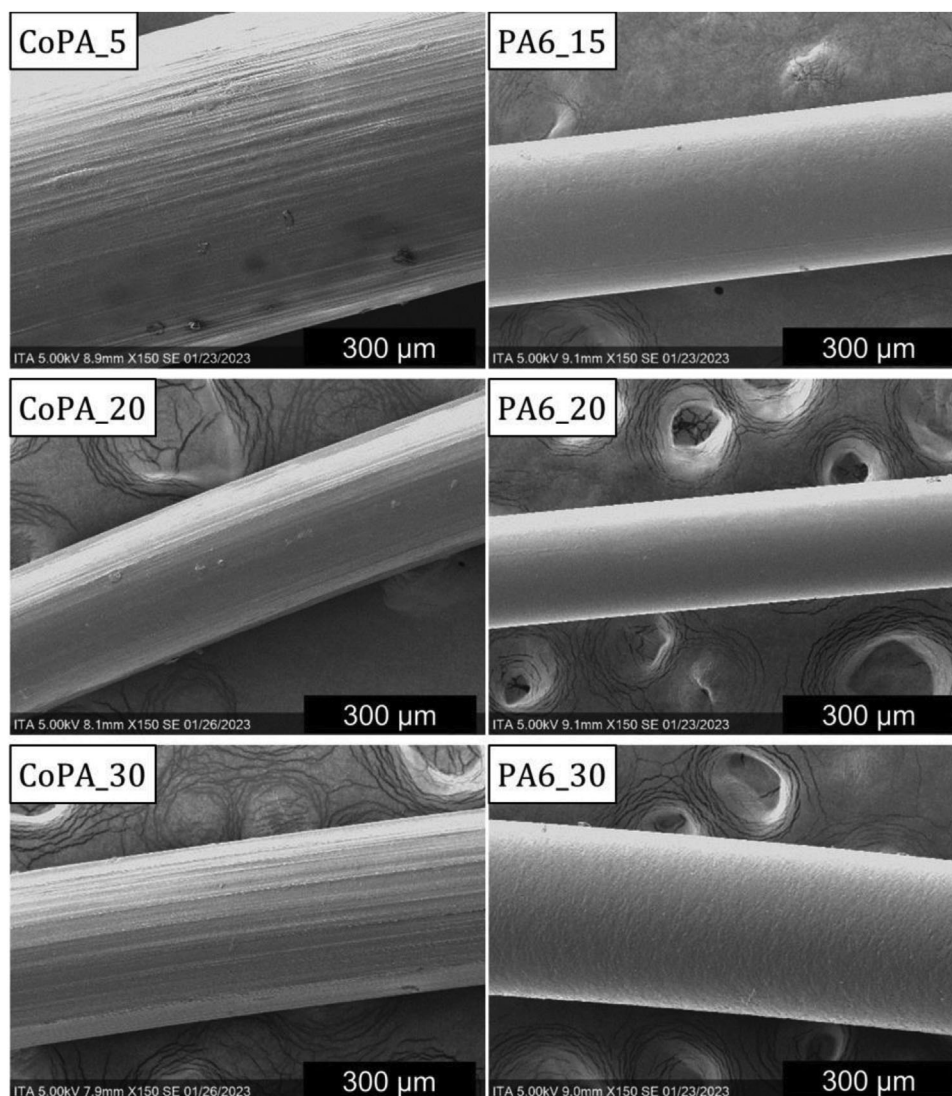
Figure 7. SEM pictures of produced monofilaments at different wind up speeds.
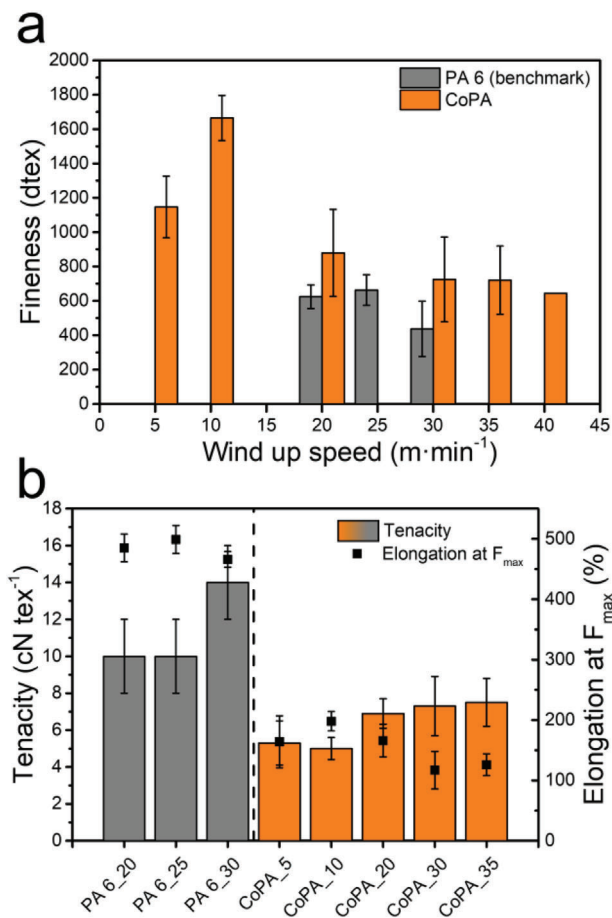
Figure 8. a) Fineness of melt-spun monofilaments in relation to the wind up speed. b) Tenacity and elongation at maximum force (F_{max}) of the melt-spun monofilaments.
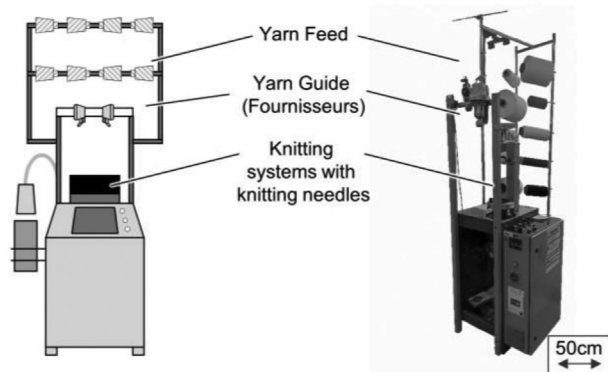
Figure 9. Small circular knitting machine used for the production of knitted fabrics.

knitting process the yarns are formed to loops interlinked to each other, forming a flexible and adaptive textile.[31]

The spun monofilament yarns of PA 6 and CoPA were processed on a laboratory circular knitting machine with a fineness of E16 (16 needles per inch) (**Figure 9**). Due to the equipped fineness of the knitting machine and knitting needles used, only the

monofilament yarns made from PA 6 and the finer yarns of the bio-based CoPA_30–40 could be processed. A courser knitting machine would be required for knitting of the thicker yarns. Nevertheless, the processability respectively knittability of the commercial PA 6 and the bio-based CoPA_30 was investigated. In general, all yarns used were knittable with the given parameters, although a major difference in the knitting loop build-up was observed.
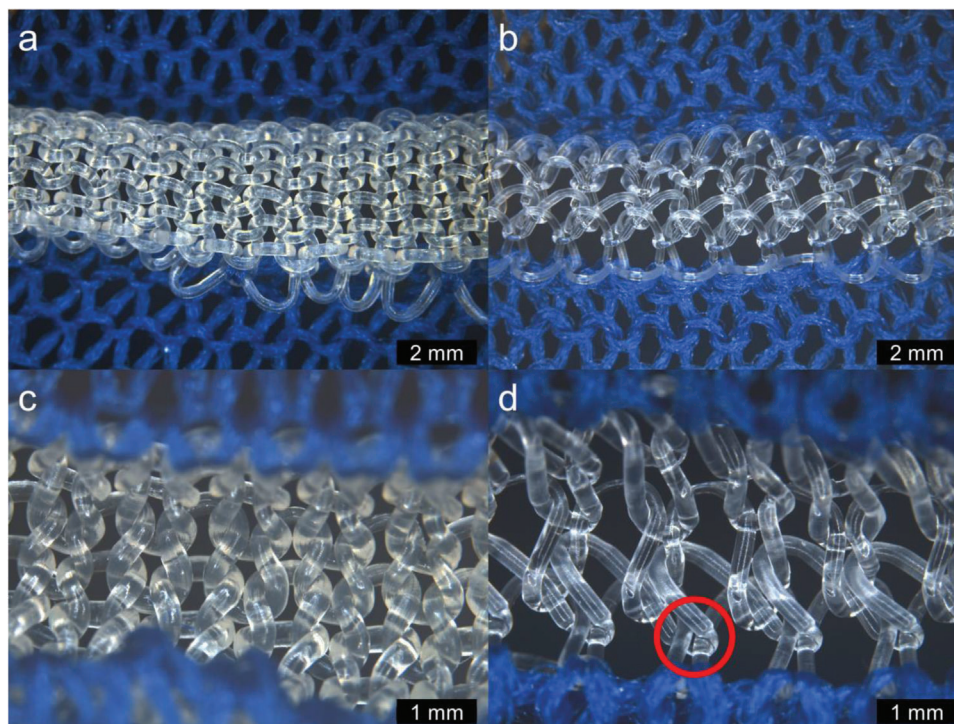
During processing of the monofilaments from commercial PA 6, the material was visibly deformed to form the loops of the knitted textile (**Figure 10**d, red circle). In contrast, the monofilaments made from the bio-based CoPA did not show any deformation (Figure 10a,c). Such deformations occur due to the take down force of the knitting needle forming the knitted loop if the material still exhibits plastic deformation properties at low elongations. Since the CoPA does not deform during knitting, plastic deformation at low elongations is not present, thus making it in principle suitable for use in the textile industry. Given that the knitting process was only carried out with laboratory spun monofilaments, the generalization of the results is not necessarily given, but gives a first good indication.

3. Conclusion

Bio-based copolymers were synthesized from oleic acid by isomerizing methoxycarbonylation and melt polycondensation with adipic acid and hexamethylene diamine in bulk. The PA 6.6/6.19 copolymers were successfully obtained with number average molecular weights suitable for melt processing applications (28 600–59 500) and in high yields. Their melting temperature could be controlled by the PA 6.6 content between 177 and 259 °C. The copolymers showed an improvement in mechanical properties compared to the PA 6.19 homopolymer. Thus, the tensile strength was improved by 58% and the Young's modulus by 28%. Surprisingly, the elongation at break was not affected by the increasing PA 6.6 content up to 64 mol%, and remained between 170 and 200%. This resulted in a large increase in toughness of the copolymers, with the copolymers having 55 and 64 mol% PA 6.6 exhibiting similar toughness (94 MPa and 92 MPa) as the commercial PA 6 (92 MPa) with a carbon-based bio-content of 33% and 26% respectively. The bio-based copolymers also exhibit four times lower water absorption than the commercial PA 6, due to the long methylene chains. Their viscoelastic properties suggest good spinnability, which was further evidenced by melt spinning of the exemplary PA 6.6/6.19 55:45 copolymer. Draw-down ratios of up to 110 could be achieved, indicating the suitability of the material for industrial spinning trials. The resulting monofilaments were also successfully knitted on a circular knitting machine to produce fabrics, further underlining the suitability of these copolymers for the production of textiles.

Surely, the copolymerization of bio-based and fossil-based monomers opens for copolyamides with tailored property profiles compromising the lack of performance of many bio-based polyamides and lack of sustainability of high-performance fossil-based polyamides. There is still plenty of room to further tune the property of copolyamides of these types of copolyamides by control of the macromolecular structure. Nevertheless, it is important at this stage, to show also potential for applications which will require the engineering input as well.

**ADVANCED
SCIENCE NEWS**

www.advancedsciencenews.com

**[M] acro-
molecular**

Rapid Communications

www.mrc-journal.de

Figure 10. Microscope images of knitted fabrics of a,c) CoPA_30 and b,d) PA 6_25.

4. Experimental Section

Materials: Oleic acid (99%) was purchased from Jinan Boss Chemical Industry Co., Ltd. 1,2-Bis(di-*tert*-butylphosphinomethyl)benzene was purchased from Henan Allgreen Chemical Co., Ltd. Methyl formate (97%) and hexamethylene diamine (99.5+%) were purchased from Acros. Methanesulfonic acid (>99%) was purchased from TCI Chemicals. Palladium(II)acetylacetonate (99%) was purchased from Sigma-Aldrich. 1,1,1,3,3,3-Hexafluoro-2-propanol (99%) was purchased from Fluorochem Ltd. Potassium hydroxide (>85%) was purchased from Carl Roth. Deuterated chloroform (CDCl$_3$, 99.8%) and dimethyl sulfoxide (DMSO-d_6, 99.8%) were purchased from Deutero. Aqueous hydrochloric acid (37%) was purchased from VWR. PA 6.6-salt and PA 6 Ultramid B24 N 03 was kindly provided by BASF. All solvents for purification were purchased in technical grade from local suppliers.

Purifications: Methyl formate was degassed by freeze-pump-thaw and stored over molecular sieves 4 Å. Methanol was dried by refluxing with calcium hydride, distilled and stored over molecular sieves 3 Å. Hexamethylene diamine was distilled and stored under argon atmosphere.

Size exclusion Chromatography: The number and weight average molar masses and molar mass distributions were measured on a 1200 Infinity (Agilent Technologies/Gynotek) gel permeation chromatography (SEC). The instrument was equipped with a PFG 7 µm precolumn and two main columns (PFG 7 µm 100 Å and PFG 7 µm 300 Å) (PSS, Mainz, Germany). A refractive index detector (RI, Gynotek SE-61) was used for the detection. The samples were dissolved in HFIP (HPLC grade) with potassium trifluoroacetate (8 mg mL^{-1}) and toluene (HPLC grade) as an internal standard in a concentration of 2 mg mL^{-1} and filtered through a 0.22 µm PTFE filter. 20 µL of this solution were injected and measured at a flow rate of 0.5 mL min^{-1} at 23 °C. Calibration of the system was performed with Poly(methyl methacrylate) (PSS calibration kit, PSS, Mainz, Germany) in a range of 1720–189 000 Da.

Nuclear Magnetic Resonance Spectroscopy (^{1}H-NMR): ^{1}H-NMR spectra were recorded using a Ultrashield-300 spectrometer (Bruker) at 300 MHz in HFIP with added CDCl$_3$ as an internal reference, for the polymers, and DMSO-d_6 or CDCl$_3$ for the monomers.

Thermal Properties: Studies on the thermal stability were performed with thermogravimetric analysis (TGA) on a TG 209 F1 Libra (Netzsch). ≈5 mg of the sample was weighed in an aluminum crucible with a pierced lid (Thepro). Dynamic measurements were performed in the range of 20–600 °C using a heating rate of 20 K min^{-1} under nitrogen 5.3 and synthetic air (O2/N2, 20/80, v/v) with a flow rate of 50 mL min^{-1}. Isothermal measurements were performed for 1 h at the respective processing temperatures of the polymers (210 °C for PA 6.19; 220 °C for PA 6.6/6.19 17:83; 270 °C for 44:56; 230 °C for 55:45; 280 °C for 64:36; 300 °C for 88:12 and PA 6.6) under nitrogen 5.3 and synthetic air (O2/N2, 20/80, v/v) with a flow rate of 50 mL min^{-1}.

Differential scanning calorimetry (DSC) was performed on a DSC 204 F1 Phoenix (Netzsch). ≈5 mg of the sample were weighed in a 30/40 µL aluminum crucible with a pierced lid (Thepro). Dynamic measurements were performed in the range of 0–350 °C at a heating rate of 20 K min^{-1} under nitrogen 5.3 with a flow rate of 20 mL min^{-1}.

Dynamic Mechanical Analysis (DMA) was performed on a DMA 1 STARe System (Mettler Toledo) in single cantilever modus. The measurements were conducted with a heating rate of 2 K min^{-1} and a frequency of 2 Hz.

Rheology: Test specimens for the rheology were produced with a 25-12-2HC hot press (Carver). The polymers were dried in a vacuum at 80 °C overnight and pressed in between two stainless steel plates separated by Kapton sheets using a circular mold with $d = 25$ mm and $h = 1$ mm at a temperature of $T_m + 30$ K for 5 min. The pressure was increased from 0 to 5 t after 2 min and held for 2 min. Thermal quenching was performed directly afterward on a LaboPress P150H manual lever cold press (Vogt Maschinenbau, Berlin, Germany) until room temperature was reached. Rheology measurements were performed on a MCR302 Rheometer (Anton Paar) using an electrical plate (P-ETD400 and an electrical hood (H-ETD400) in parallel plate geometry with $d = 25$ mm. The dynamic measurements were conducted isothermal at 2% deformation and the shear rate was varied between 100 and 0.631 rad s^{-1}.

**ADVANCED
SCIENCE NEWS**

www.advancedsciencenews.com

Macro-
molecular
Rapid Communications

www.mrc-journal.de

Mechanical Properties of the Polymers: The mechanical properties of the bulk materials were determined by uniaxial stress–strain testing on a BT1-FR 0.5TND14 (Zwick/Roell) at room temperature. The test specimens of type 5B according to DIN EN ISO 527-2 were produced by injection molding on a Micro Injector 5000 (DACA Instruments) with 5 mL barrel-volume. The dimensions of the test specimens were measured at one sample for each nest with a Series 293 (0–25 mm) digital micrometer (Mitutoyo, Neuss, Germany), taking the average of three different positions in the gauge area. The specimens were dried for 48 h at 80 °C under applied vacuum prior to testing. Tensile tests were performed according to DIN EN ISO 527 at 50 mm min^{-1} at a grip to grip separation of 20 mm. The Young's modulus was determined by the slope of the linear region of the stress–strain curves in range of 0.05%–0.25% deformation. At least seven specimens were tested for each material and the statistical average is given as a result.

Water Uptake: The water uptake tests of the polyamides were performed in triplicate according to DIN EN ISO 62. Disc-shaped test specimens with $d = 25$ mm and $h = 1$ mm were produced via melt pressing analogous to the rheology test specimens. The test specimens were dried in a vacuum oven at 80 °C for 48 h prior to testing and weighed after cooling to room temperature in a desiccator to determine the initial weight (m_0). The specimens were then immersed in deionized water at room temperature for 7 days. Prior to weighing (m_t), the samples were thoroughly dried with a cloth to remove any surface water. The water uptake was determined using Equation (1):

$$\text{water uptake} = \frac{m_t - m_0}{m_0} \cdot 100\% \tag{3}$$

Crystal Structure: The analysis of the crystal structure of the polyamides was performed using an X-ray diffraction on a D8 ADVANCE diffractometer (Bruker), equipped with Cu Kα radiation ($\lambda = 0.154$ nm). The source was operated at 40 kV and 40 mA and measurements were recorded in a 2θ range of 5–40° with a step-size of 0.025° min^{-1} at room temperature. Disc-shaped test specimens with $d = 25$ mm and $h = 1$ mm were produced via melt pressing analogous to the rheology test specimens.

Scanning Electron Microscopy: Scanning electron microscopy of the monofilaments was performed using a FlexSEM 1000 II (Hitachi High-Tech Corporation) with an acceleration voltage of 5 kV at high vacuum. The samples were sputtered with gold and the pictures were recorded in secondary electron (SE) mode.

Monofilament Characterization: The fineness of the monofilaments was analyzed according to DIN 53830–3. The monofilaments were tested under norm climate with 25 h of acclimatization in accordance with DIN EN ISO 139. 100 mm samples were analyzed in triplicate with a pre-tension of 0.5 cN tex^{-1}.

Tensile tests of the monofilaments were performed according to DIN EN 13 895 on a Statimat 4U (Textechno Herbert Stein GmbH und Co. KG) using a sample length of 100 mm at 100 mm min^{-1} testing speed and a pre-tension of 0.5 cN tex^{-1}. 10 specimens were tested for each material and the statistical average is given as a result.

Synthesis of Dimethyl-1.19-Nonadecanedionate: The synthesis of dimethyl-1.19-nonadecanedionate was performed as previously reported.[16] All steps were performed under inert gas atmosphere. 121 mg (0.40 mmol, 4 mol%) palladium(II)acetylacetonate and 627.0 mg (1.59 mmol, 1.6 mol%) 1,2-Bis(di-*tert*-butylphosphino-methyl)benzene (dtbpx) were weighed into a 250 mL stainless steel autoclave equipped with a stirring bar. A solution of 28.04 g (99.27 mmol) oleic acid, 99%, 48 mL methyl formate and 154 μL (2.38 mmol, 6 mol%) methanesulfonic acid (MSA) in 48 mL methanol was prepared and directly transferred into the autoclave using a syringe under inert gas counterflow. The autoclave was closed and heated to 100 °C while stirring for 24 h. During this period, the pressure gradually increased to 6–12 bar. After cooling the autoclave to room temperature, the pressure was carefully released. The reaction products were washed out of the autoclave with 2 × 40 mL methylene chloride. The resulting yellow solution was filtered over neutral Al$_2$O$_3$ to remove possible Pd black and excess catalyst. The solvent was removed

using a rotary evaporator to yield the crude product as yellow crystals. These were purified by two times recrystallization from 200 mL methanol to isolate the 1.19-nonadecanedionate **2** as white crystals with a purity of >99% (GC) and a yield of 80%.

^{1}H-NMR: (300 MHz, CDCl$_3$, 298 K, δ): 3.66 (s, 6H, O-CH$_3$, 2.30 (t, $J =$ 7.6 Hz, 4H, CH$_2$), 1.61 (m, 4H, CH$_2$), 1.25 (m, 26H, CH$_2$).

Synthesis of 1.19-Nonadecanedioic Acid: The synthesis of 1.19-nonadecanedioic acid was performed as previously reported.[16] 24.5 g (68.6 mmol) dimethyl-1.19-nonadecanedionate were transferred into a 1 L round bottom flask equipped with a large stirring bar. A solution of 46.2 g potassium hydroxide in 462 mL methanol was added to the flask and heated to 85 °C while stirring for 12 h to form a white slurry. After cooling to room temperature, the solvent was removed in vacuo to yield the potassium salt as white solids. The salt was then dissolved in 236 mL deionized water followed by slow addition of aqueous hydrochloric acid (6 m) until pH≈1, resulting in a white precipitate. The precipitate was washed neutral with deionized water and then dried for 24 h at 80 °C to obtain the pure 1.19-nonadecanedioic acid as white solids in a yield of 22.5 g (68.4 mmol, 99% yield).

^{1}H-NMR: (300 MHz, DMSO-d_6, 298 K, δ): 11.98 (s, 2H, COOH), 2.18 (t, $J =$ 7.3 Hz, 4H, CH$_2$), 1.47 (m, 4H, CH$_2$), 1.23 (s, 26H, CH$_2$).

Synthesis of Copolymers: The PA-salts of PA 6.19 and PA 6.6 were prepared by dissolving equimolar amounts of hexamethylene diamine and 1.19-diacid or adipic acid respectively in ethanol for PA 6.19 or water for PA 6.6 to form solutions of 10 wt%. Complete dissolution of the diacid was achieved by heating to 80 °C. Upon complete dissolution, the diamine-solution was added, causing the formation of the PA-salt as a white precipitate. After another 2 h of heating the solution was cooled to room temperature. The formed PA-salt was recovered by filtration and washed with warm ethanol respectively water to yield the desired PA-salts in ≈90 % yield.

For the synthesis of PA 6.6/6.19 copolymers the PA-salts of PA 6.6 and PA 6.19 were mixed in the desired ratio with a spatula. This mixture was then transferred into a three-necked Schlenk-tube with a mechanical stirrer and distillation bridge attached. Upon exchange of atmosphere with argon to ensure exclusion of oxygen the mixture was heated to 160 °C under stirring. The temperature was increased stepwise in 10 K increments to ensure melting until the final temperature of 265 °C is reached within 4 h. Then the temperature was held at 265 °C for 3 h under stirring. Afterward vacuum was applied to ensure complete evaporation of water and the reaction proceeded for another 2 h. Then the tube was vented with argon and cooled to room temperature. The formed polymer was dissolved in HFIP (hexafluoro isopropanol) and recovered by precipitation in methanol. After drying the overall yield of recovered polymer was ≈90%.

Melt Spinning: Melt spinning of the polyamides was performed using a MC 15 HT micro compounder (Xplore Instruments BV) with a batch-wise manual polymer feed and a twin-screw setup. A monofilament spinneret hole with a diameter of 3 mm was used and the take-up godet served as the winder. The polymers were dried prior to processing at 80 °C under applied vacuum overnight. The residual moisture content was determined by Karl Fischer titration using a C30 Coulometric Karl Fischer titrator (Mettler-Toledo).

Knitting Trials: The melt-spun monofilaments were processed on a laboratory circular knitting machine TK 83 (Maschinenfabrik Harry Lucas GmbH & Co. KG), with a fineness of E16 (16 needles per inch). The yarn feeding was controlled by a EFS 820 Fournisseur (Memminger-Iro GmbH) to maintain a constant yarn tension of 1.5 cN.

Supporting Information

Supporting Information is available from the Wiley Online Library or from the author.

Acknowledgements

2300256 (10 of 11)

**ADVANCED
SCIENCE NEWS**

www.advancedsciencenews.com

{M} acro-
molecular
Rapid Communications

www.mrc-journal.de

Conflict of Interest

The authors declare no conflict of interest.

Data Availability Statement

The data that support the findings of this study are available in the supplementary material of this article.

[1] E. Commission, *Publications Office* **2019**.
[2] TextileExchange, Preferred Fiber & Materials, https://textileexchange.org/wp-content/uploads/2021/08/Textile-Exchange_Preferred-Fiber-and-Materials-Market-Report_2021.pdf, accessed: 08.2022.
[3] M. Winnacker, B. Rieger, *Macromol. Rapid Commun.* **2016**, *37*, 1391.
[4] R. Hufenus, Y. Yan, M. Dauner, T. Kikutani, *Materials* **2020**, *13*, 4298.
[5] F. Stempfle, D. Quinzler, I. Heckler, S. Mecking, *Macromol. Chem. (Oxford)* **2011**, *44*, 4159.
[6] X. Miao, R. Malacea, C. Fischmeister, C. Bruneau, P. H. Dixneuf, *Green Chem.* **2011**, *13*, 2911.
[7] a) H. Mutlu, R. Hofsäß, R. E. Montenegro, M. A. R. Meier, *RSC Adv.* **2013**, *3*, 4927; b) X. Li, J. Choo Ping Syong, Y. Zhang, *Green Chem.* **2018**, *20*, 3619; c) R. S. Atapalkar, P. R. Athawale, D. Srinivasa Reddy, A. A. Kulkarni, *Green Chem.* **2021**, *23*, 2391.
[8] a) T. Witt, F. Stempfle, P. Roesle, M. Häußler, S. Mecking, *ACS Catal.* **2015**, *5*, 4519; b) G. A. Abel, K. O. Nguyen, S. Viamajala, S. Varanasi, K. Yamamoto, *RSC Adv.* **2014**, *4*, 55622.
[9] a) A. Y. Mudiyanselage, S. Viamajala, S. Varanasi, K. Yamamoto, *ACS Sustainable Chem. Eng.* **2014**, *2*, 2831; b) G. A. Abel, S. Viamajala, S. Varanasi, K. Yamamoto, *ACS Sustainable Chem. Eng.* **2016**, *4*, 5703.
[10] M. A. R. Meier, *Macromol. Rapid Commun.* **2019**, *40*, 1800524.
[11] L. Tao, K. Liu, T. Li, R. Xiao, *Polym. Bull.* **2020**, *77*, 1135.
[12] X. Cui, W. Li, D. Yan, *Polym. Int.* **2004**, *53*, 1729.
[13] a) C. Bennett, E. Kaya, A. M. Sikes, W. L. Jarrett, L. J. Mathias, *J. Polym. Sci., Part A: Polym. Chem.* **2009**, *47*, 4409; b) C. Bennett, L. J. Mathias, *J. Polym. Sci., Part A: Polym. Chem.* **2005**, *43*, 936; c) C. Bennett, L. J. Mathias, *Macromol. Chem. Phys.* **2004**, *205*, 2438; d) X. Cui, W. Li, D. Yan, C. Yuan, G. Di Silvestro, *J. Appl. Polym. Sci.* **2005**, *98*, 1565.
[14] D. Pingen, J. B. Schwaderer, J. Walter, J. Wen, G. Murray, D. Vogt, S. Mecking, *ChemCatChem* **2018**, *10*, 3027.
[15] B. Cornils, P. Lappe, in *Ullmann's Encyclopedia of Industrial Chemistry*, 7th ed., Wiley-VCH, Weinheim **2010**.
[16] M. Rist, A. Greiner, *ACS Sustainable Chem. Eng.* **2022**, *10*, 16793.
[17] Q. Guo, C. Fan, H. Liu, Y. Cai, *Polym. Polym. Compos.* **2011**, *19*, 69.
[18] F. Jia, J.-L. Mao, X.-Y. Yang, Y. Ma, C. Yao, *Chin. Chem. Lett.* **2013**, *24*, 654.
[19] F. Jia, J. L. Mao, Y. Ma, C. Yao, *J. Appl. Polym. Sci.* **2014**, *131*, 39845.
[20] P. Zierdt, E. Mitzner, A. Gomoll, T. Theumer, A. Lieske, *J. Appl. Polym. Sci.* **2016**, *133*, 44155.
[21] T. Elzein, M. Brogly, J. Schultz, *Kobunja Kwahak Kwa Kisul* **2002**, *43*, 4811.
[22] S. Koltzenburg, M. Maskos, O. Nuyken, *Polymere: Synthese, Eigenschaften und Anwendungen*, Springer, Berlin, Heidelberg **2014**.
[23] M. Ehrenstein, S. Dellsperger, C. Kocher, N. Stutzmann, C. Weder, P. Smith, *Kobunja Kwahak Kwa Kisul* **2000**, *41*, 3531.
[24] Y. Li, G. Yang, *Macromol. Rapid Commun.* **2004**, *25*, 1714.
[25] M. Winkler, M. A. R. Meier, *Green Chem.* **2014**, *16*, 1784.
[26] a) I. Clavería, D. Elduque, J. Santolaria, C. Pina, C. Javierre, A. Fernandez, *Polym. Test.* **2016**, *50*, 15; b) V. Venoor, J. H. Park, D. O. Kazmer, M. J. Sobkowicz, *Polym. Rev.* **2021**, *61*, 598.
[27] a) F. Fourné, *Synthetic fibers: Machines and equipment, manufacture, properties*, Hanser, Munich **1999**; b) Z. K. Walczak, *Processes of fiber formation*, 1st ed., Elsevier, Amsterdam, New York **2002**.
[28] a) P. J. Carreau, D. C. de Kee, R. P. Chhabra, *Rheology of Polymeric Systems: Principles and applications*, 2nd ed. Carl Hanser Verlag GmbH & Co. KG, München **2021**; b) K. Yasuda, R. C. Armstrong, R. E. Cohen, *Rheol. Acta* **1981**, *20*, 163.
[29] T. A. Osswald, N. Rudolph, *Polymer Rheology: Fundamentals and applications*, Hanser, Munich, Cincinnati **2015**.
[30] R. Beyreuther, R. Vogel, *Int. Polym. Proc.* **1996**, *11*, 154.
[31] T. Gries, D. Veit, B. Wulfhorst, *Textile Technology: An Introduction*, 2nd ed. Hanser, Munich, Cincinnati, Ohio **2017**.